

## TCAD modeling of radiation-induced defects in 4H-SiC diodes

Philipp Gaggl<sup>a,b</sup>, Jürgen Burin<sup>a</sup>, Andreas Gsponer<sup>a,b</sup>, Simon Emanuel Waid<sup>a</sup>, Richard Thalmeier<sup>a</sup>, Thomas Bergauer<sup>a,\*</sup>

<sup>a</sup>Institute of High Energy Physics of the Austrian Academy of Sciences, Nikolsdorfer Gasse 18, 1050, Vienna, Austria

<sup>b</sup>TU Wien, Wiedner Hauptstr. 8–10, 1040, Vienna, Austria

---

arXiv:2407.11776v3 [physics.ins-det] 5 Nov 2024

### Abstract

4H silicon carbide (SiC) has several advantageous properties compared to silicon (Si) making it an appealing detector material, such as a larger charge carrier saturation velocity, bandgap, and thermal conductivity. While the current understanding of material and model parameters suffices to simulate unirradiated 4H-SiC using TCAD software, configurations accurately predicting performance degradation after high levels of irradiation due to induced traps and recombination centers do not exist. Despite increasing efforts to characterize the introduction and nature of such defects, published results are often contradictory. This work presents a bulk radiation damage model for TCAD simulation based on existing literature and optimized on measurement results of neutron-irradiated 4H-SiC pad diodes. Experimentally observed effects, such as flattening of the detector capacitance, loss of rectification properties, and degradation in charge collection efficiency, are reproduced. The  $\text{EH}_4$  center is suggested as a major lifetime killer in 4H-SiC, while the still controversial assumption of the  $\text{EH}_{6,7}$  deep-level being of donor type is reinforced.

**Keywords:** Silicon carbide, Radiation damage to detector materials (solid state), TCAD, Numerical simulations, Defect states

---

### 1. Introduction

Future high-energy physics (HEP) experiments ought to sustain unprecedented radiation fluences up to  $10^{18} \text{ n}_{\text{eq}}/\text{cm}^2$  (1 MeV neutron equivalent according to NIEL hypothesis [1]) at innermost detector layers, while low material budget requirements forbid materials like cooling pipes. Due to its unique properties and recent improvements in manufacturing, research in 4H silicon carbide (4H-SiC) as high-energy particle detector material has been rekindled [2, 3]. A venture necessitating simulations via technology computer-aided design (TCAD) software. Despite a multitude of studies on performance degradation of, and defect formation in 4H-SiC after irradiation, no TCAD model to accurately reproduce these findings exists to the best of our knowledge. Utilizing the TCAD software Sentaurus [4], this work represents our first results towards developing a comprehensive radiation damage model for 4H-SiC up to high irradiation fluences. Focused solely on bulk defects, literature defect parameters are adapted to reproduce measurements on neutron-irradiated 4H-SiC samples described in [5].

### 2. Materials and methods

Five planar,  $3 \times 3 \text{ mm}^2$  4H-SiC PiN-diodes with a  $50 \mu\text{m}$ , high resistive ( $20 \Omega \text{ cm}$ ), epitaxial layer as active detecting region, manufactured and developed at IMB-CNM-CSIC [6], were studied. Four of them were neutron-irradiated at the TRIGA Mark II reactor at the Atominstut in Vienna at different fluences ( $\Phi$ ), ranging from  $5 \times 10^{14} \text{ n}_{\text{eq}}/\text{cm}^2$  to  $1 \times 10^{16} \text{ n}_{\text{eq}}/\text{cm}^2$ . Detailed information can be found in [7]. The electrical characterization included current (I-V) and capacitance (C-V), as well as charge collection efficiency (CCE) measurements of  $\alpha$ -particles in forward and reverse operating bias [5]. Due to the  $\text{p}^{++}$ -implant and metalization covering the active diode area, the proposed TCAD model considers only bulk defects, neglecting contributions of interface defects and oxide charges. Results of existing literature characterizing radiation-induced defects in 4H-SiC are subject to differing manufacturers and material quality, thus widely dispersed and sometimes contradictory. The ensuing large parameter space served as a starting point for the optimization of individual values to best fit experimental results from [5]. The investigated publications focus on neutron and electron-irradiated 4H-SiC since results compare very well [8, 9, 10]. Active defects in the simulation are either intrinsic (D & B) or radiation-induced ( $\text{Z}_{1,2}$ ,  $\text{EH}_{6,7}$  &

---

\*Corresponding author

Email address: thomas.bergauer@oeaw.ac.at (Thomas Bergauer)

EH<sub>4</sub>) via a linear introduction rate ( $N_i = f_i \cdot \Phi$ ). Defect types and cross-sections are assumed constant over the whole range of neutron fluences. Due to the low dark current levels of 4H-SiC, reverse I-V measurements are dominated by electric noise and surface currents, restricting TCAD comparison to forward bias operation. I-V simulations have been conducted in *SDevice*, using an AC Analysis in *Single-Device Mode* to simultaneously obtain C-V data (10 kHz AC-frequency [5]) at equal simulation settings. Obtained field constellations were saved in 50 V steps and used to simulate detection performance, utilizing the *HeavyIon* model to simulate the depth-dependent energy loss of  $\alpha$ -particles corresponding to the source used in [5]. Applied settings and physics models are described in [11, 12, 13].

### 3. Results

Table 1 summarizes the optimized defects of the TCAD irradiation model and their respective parameters, as well as publications best fitting the final obtained values. Aside from the widely known *major lifetime killers* in 4H-SiC (Z<sub>1,2</sub> & EH<sub>6,7</sub>), the EH<sub>4</sub> defect cluster proved to be crucial as well. As discussions about the type of the EH<sub>6,7</sub> defect continue, the presented model strongly suggests it to be of donor-type [14, 15]. Aside from slight improvements in C-V conformity, the intrinsic Boron centers (B & D) do not affect results.

Table 1: Optimized TCAD model parameters: Defect type, activation energy,  $e^-/h^+$  capture cross-sections, and concentration after 1 MeV equivalent neutron fluence  $\Phi$ .  $E_C$  and  $E_V$  denote the conduction and valence band energy. Additionally, the investigated literature that best fits the respective value, is given.

Defect	Type	$E$ [eV]	$\sigma_e$ [cm <sup>2</sup> ]	$\sigma_h$ [cm <sup>2</sup> ]	$N$ [cm <sup>-3</sup> ]
Z <sub>1,2</sub>	Acceptor	$E_C - 0.67$ [16]	$2.0 \cdot 10^{-14}$ [16]	$3.5 \cdot 10^{-14}$ [17]	$5.0 \cdot \Phi$ [8]
EH <sub>6,7</sub>	Donor	$E_C - 1.60$ [18]	$9.0 \cdot 10^{-12}$ [18]	$3.8 \cdot 10^{-14}$ [18]	$1.6 \cdot \Phi$ [8]
EH <sub>4</sub>	Acceptor	$E_C - 1.03$ [19]	$5.0 \cdot 10^{-13}$ [20]	$5.0 \cdot 10^{-14}$ [8]	$2.4 \cdot \Phi$ [8]
B	Donor	$E_V + 0.28$ [21]	$2.0 \cdot 10^{-15}$ [22]	$2.0 \cdot 10^{-14}$ [8]	$1.0 \cdot 10^{14}$
D	Donor	$E_V + 0.54$ [21]	$2.0 \cdot 10^{-15}$ [22]	$2.0 \cdot 10^{-14}$ [8]	$1.0 \cdot 10^{14}$

Figure 1 depicts measured and simulated I-V results in forward bias. The model accurately predicts the 4H-SiC device losing its rectifying properties with increasing irradiation, allowing for forward biasing up to high voltages [5, 10]. Absolute values are in good agreement with experiments, despite increasingly underestimating current levels with rising fluence, which may be attributed to surface currents omitted in the model. Simulations suggest a high concentration of trapped holes (EH<sub>6,7</sub>) near the top, and electrons (EH<sub>4</sub>) near the bottom due to their respective abundance within the p<sup>++</sup> implant and the n<sup>+</sup> buffer layer [6]. The resulting potential forms an electric field barrier that suppresses current flow and increases with the irradiation fluence. The current level in this confinement is mainly determined by the majority carrier trap (Z<sub>1,2</sub> & EH<sub>4</sub>) concentration. At sufficient bias, defects on either side become fully occupied, increasing the respective carrier lifetimes and restoring conducting properties, as can be observed for the lowest fluence in Figure 1. The resulting rectification voltage is determined by the EH<sub>4</sub> concentration, as it reaches full occupations earlier. Not displayed are reverse I-V simulations, which show a slight increase in leakage current with irradiation fluence that remains below an order of magnitude increase. Although in agreement

with other studies [7, 10], no further conclusion can be made, as simulated currents are multiple orders of magnitude below the experimental measurement limitations of around 100 fA.

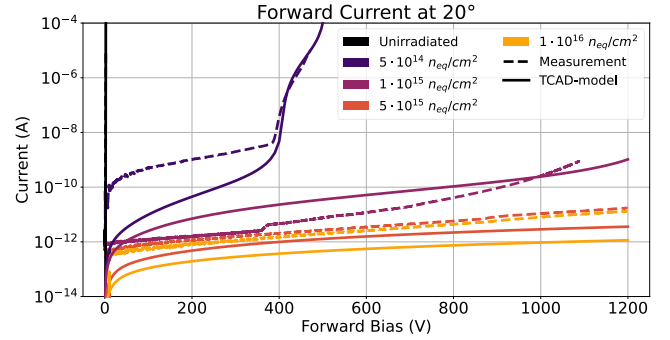


Figure 1: Forward bias I-V measurements [5] vs. simulation.

The detector capacitance has been shown to *flatline* after irradiation, adopting a constant value across forward and reverse bias [5, 10]. Figure 2 displays measured and simulated reverse  $1/C^2$  data. While defect parameters were adjusted mainly to agree with I-V measurements, C-V simulations reproduce experimental results, with slight deviations most likely originating in inaccuracies in the simulated initial doping profile.

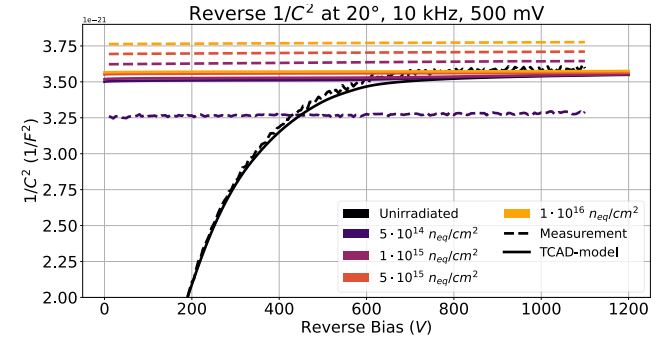


Figure 2: Reverse bias  $1/C^2$ -V measurements [5] vs. simulation. The unirradiated case (black) represents the characteristic depletion of a PiN-diode under reverse operation, the extracted full depletion voltage is 325 V.

Measured and simulated charge collection efficiency (CCE), obtained by scaling signal areas to that of the unirradiated counterpart, are shown in Figure 3. The radiation-induced performance degradation can be reproduced well at low irradiation, while deviations increase towards higher fluences.

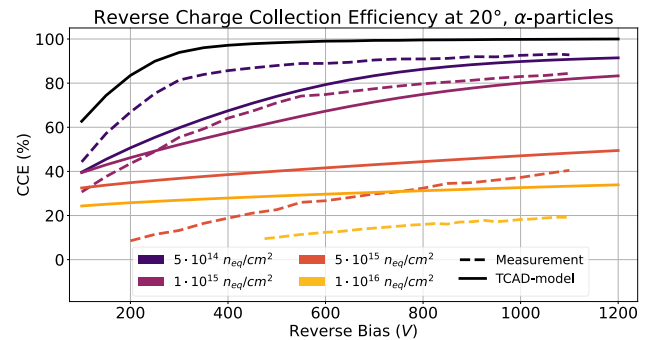


Figure 3: Reverse bias CCE measurements [5] vs. simulation.

## 4. Conclusions and Outlook

A first step towards a comprehensive TCAD model for radiation-induced bulk defects in 4H-SiC has been developed. Simulated data agrees well with measurements on neutron-irradiated 4H-SiC diodes. While absolute I-V values deviate with increasing irradiation fluence, the loss of rectification properties after irradiation can be reproduced. Suggested to be originating from major shifts within the internal electric field structure due to charge separation, the deep-level defects EH<sub>4</sub> and EH<sub>6,7</sub> are identified as driving forces behind this process. Furthermore, the model reinforces recent and still discussed proposals of the EH<sub>6,7</sub> center being of donor type while also introducing the EH<sub>4</sub> defect as a significant lifetime killer in 4H-SiC, next to the established Z<sub>1,2</sub> center. Other trends, such as a flattening detector capacitance and a degradation in charge collection efficiency after irradiation, are recreated and agree well with experimental results at lower fluences, increasingly deviating at higher fluences. Further and more extensive irradiation studies on various types of 4H-SiC devices are needed to confirm and improve the presented simulation model, as well as to expand it towards interface defects and oxide charges. Additional 4H-SiC samples, currently under production, are scheduled for an extensive irradiation campaign, which will include various irradiation sources and is planned to cover a wide fluence range of 10<sup>13</sup> n<sub>eq</sub>/cm<sup>2</sup> to 10<sup>18</sup> n<sub>eq</sub>/cm<sup>2</sup>.

## Acknowledgements

This project has received funding from the Austrian Research Promotion Agency FFG, grant numbers 883652 and 895291. Production and development of the 4H-SiC samples was supported by the Spanish State Research Agency (AEI) and the European Regional Development Fund (ERDF), ref. RTC-2017-6369-3.

## References

- [1] M. Moll, Radiation Damage in Silicon Particle Detectors: Microscopic defects and macroscopic properties, Ph.D. thesis, Hamburg U., 1999.
- [2] J. Coutinho, et al., Silicon carbide diodes for neutron detection, NIM-A 986 (2021) 164793.
- [3] F. Nava, et al., Silicon carbide and its use as a radiation detector material, Measurement science & technology 19 (2008) 102001.
- [4] Synopsys Sentaurus TCAD Ver. V-2023.09, Synopsys, Inc., 2024. URL: <https://www.synopsys.com/home.aspx>.
- [5] A. Gsponer, et al., Neutron radiation induced effects in 4H-SiC PiN diodes, JINST 18 (2023). doi:10.1088/1748-0221/18/11/C11027.
- [6] J. Rafi, et al., Four-quadrant silicon and silicon carbide photodiodes for beam position monitor applications: electrical characterization and electron irradiation effects, JINST 13 (2018). doi:10.1088/1748-0221/13/01/C01045.
- [7] P. Gaggl, et al., Charge collection efficiency study on neutron-irradiated planar silicon carbide diodes via UV-TCT, NIM-A 1040 (2022). doi:10.1016/j.nima.2022.167218.
- [8] P. Hazdra, et al., Point Defects in 4H-SiC Epilayers Introduced by 4.5 MeV Electron Irradiation and their Effect on Power JBS SiC Diode Characteristics, in: Gettering and Defect Engineering in Semiconductor Technology XV, volume 205 of *Solid State Phenomena*, Trans Tech Publications Ltd, 2014, pp. 451–456. doi:10.4028/www.scientific.net/SSP.205-206.451.
- [9] P. Hazdra, J. Vobecký, Radiation Defects Created in n-Type 4H-SiC by Electron Irradiation in the Energy Range of 1–10 MeV, physica status solidi (a) 216 (2019) 1900312. doi:<https://doi.org/10.1002/pssa.201900312>.
- [10] J. M. o. Rafi, Electron, Neutron, and Proton Irradiation Effects on SiC Radiation Detectors, IEEE Transactions on Nuclear Science 67 (2020) 2481–2489. doi:10.1109/TNS.2020.3029730.
- [11] P. Gaggl, Improving TCAD simulation of 4H silicon carbide particle detectors, presented at 42rd RD50 workshop, CERN, Switzerland, <https://indico.cern.ch/event/1334364/contributions/5672054/>, 2023.
- [12] Synopsys Sentaurus TCAD, Tips & Tricks 2. Simulating Wide-Bandgap Semiconductors With Sentaurus Device, [https://spdocs.synopsys.com/dow\\_retrieve/qsc-r/seg/sentaurus/R-2020.09/training/sentaurus\\_training/tips/tips\\_2.html](https://spdocs.synopsys.com/dow_retrieve/qsc-r/seg/sentaurus/R-2020.09/training/sentaurus_training/tips/tips_2.html), 2020.
- [13] Synopsys Sentaurus TCAD, Sentaurus Device 15. Special Focus: 4H-SiC PiN Device Breakdown Simulation, [https://spdocs.synopsys.com/dow\\_retrieve/qsc-r/seg/sentaurus/R-2020.09/training/sentaurus\\_training/sd/sd\\_15.html#5](https://spdocs.synopsys.com/dow_retrieve/qsc-r/seg/sentaurus/R-2020.09/training/sentaurus_training/sd/sd_15.html#5), 2020.
- [14] I. D. Booker, et al., Donor and double-donor transitions of the carbon vacancy related EH<sub>6,7</sub> deep level in 4H-SiC, Journal of Applied Physics 119 (2016) 235703. doi:10.1063/1.4954006.
- [15] M. E. Bathen, et al., Dual configuration of shallow acceptor levels in 4H-SiC, Materials Science in Semiconductor Processing 177 (2024) 108360. doi:<https://doi.org/10.1016/j.mssp.2024.108360>.
- [16] P. B. Klein, Identification and carrier dynamics of the dominant lifetime limiting defect in n–4H-SiC epitaxial layers, physica status solidi (a) 206 (2009) 2257–2272. doi:<https://doi.org/10.1002/pssa.200925155>.
- [17] P. B. Klein, et al., Lifetime-limiting defects in n–4H-SiC epilayers, Applied Physics Letters 88 (2006) 052110. doi:10.1063/1.2170144.
- [18] T. Knezevic, et al., Boron-Related Defects in N-Type 4H-SiC Schottky Barrier Diodes, Materials 16 (2023). doi:10.3390/ma16093347.
- [19] G. Alfieri, et al., Annealing behavior between room temperature and 2000°C of deep level defects in electron-irradiated n-type 4H silicon carbide, Journal of Applied Physics 98 (2005) 043518. doi:10.1063/1.2009816.
- [20] I. D. Booker, et al., Carrier Lifetime Controlling Defects Z1/2 and RB1 in Standard and Chlorinated Chemistry Grown 4H-SiC, Crystal Growth & Design 14 (2014) 4104–4110. doi:10.1021/cg5007154.
- [21] I. Capan, T. Brodar, Majority and Minority Charge Carrier Traps in n-Type 4H-SiC Studied by Junction Spectroscopy Techniques, Electronic Materials 3 (2022) 115–123. URL: <https://www.mdpi.com/2673-3978/3/1/11>.
- [22] P. B. Klein, et al., Slow de-trapping of minority holes in n-type 4H-SiC epilayers, physica status solidi (a) 208 (2011) 2790–2795. doi:<https://doi.org/10.1002/pssa.201127260>.